Membrane wounding triggers ATP release and dysferlin-mediated intercellular calcium signaling

J. Fernando Covian-Nares*, Srinagesh V. Koushik, Henry L. Puhl, III and Steven S. Vogel‡

Laboratory of Molecular Physiology, National Institute on Alcohol Abuse and Alcoholism, National Institutes of Health, Bethesda, MD 20892, USA

*Present address: Facultad de Ciencias Médicas y Biológicas 'Dr Ignacio Chavez', Universidad Michoacana de San Nicolás de Hidalgo, CP 58000, Morelia, Mich., Mexico

‡Author for correspondence (stevevog@mail.nih.gov)

Accepted 19 March 2010
Journal of Cell Science 123, 1884-1893

doi:10.1242/jcs.066084

Summary

Dysferlin is a Ca^{2+}-binding protein found in many different cell types. It is required for membrane wound repair in muscle, but it is not known whether it has the same function in other cells. Here we report the activation of an intercellular signaling pathway in sea urchin embryos by membrane wounding that evokes Ca^{2+} spikes in neighboring cells. This pathway was mimicked by ATP application, and inhibited by apyrase, cadmium, and ω-agatoxin-IVA. Microinjection of dysferlin antisense phosphorodiamidate morpholino oligonucleotides blocked this pathway, whereas control morpholinos did not. Co-injection of mRNA encoding human dysferlin with the inhibitory morpholino rescued signaling activity. We conclude that in sea urchin embryos dysferlin mediates Ca^{2+}-triggered intercellular signaling in response to membrane wounding.

Key words: Dysferlin, ATP, Wounding, Repair, Morpholino oligonucleotides

Introduction

In *Caenorhabditis elegans*, mutations in the gene encoding dysferlin (Fer-1) cause infertility, and in sperm dysferlin is thought to mediate vesicular membrane fusion (Washington and Ward, 2006). In cochlear hair cells a dysferlin homologue, otoferlin, is thought to mediate neurotransmitter release, and mutations in the gene encoding otoferlin cause deafness (Roux et al., 2006). In skeletal muscle, dysferlin participates in membrane wound repair mechanisms (Bansal et al., 2003), and these repair mechanisms are thought to involve membrane fusion (Bansal et al., 2003; Lennon et al., 2003). Mutations in the gene encoding dysferlin cause limb girdle muscular dystrophy-2B (LGMD2B) and Miyoshi muscular dystrophy (MMD) (Aoki et al., 2001; Bashir et al., 1994; Liu et al., 1998). At present, there are no treatments available for these muscle-wasting diseases. Accordingly, there is great interest in understanding the role dysferlin plays in wound repair. In sea urchin eggs, a widely used model system for studying plasma membrane wounding (McNeil et al., 2003; Terasaki et al., 1997), a dysferlin homolog has been identified (Sodergren et al., 2006), but its role in wound repair has never been studied.

If sea urchin dysferlin does participate in a cellular response to wounding, potentially it might act either directly or indirectly to mitigate the impact of plasma membrane wounds. In a direct role dysferlin might allow a wounded cell to survive an injury. It has been proposed that Ca^{2+} influx through a plasma membrane breach triggers dysferlin-mediated membrane fusion to seal the lesion (Bansal et al., 2003; Glover and Brown, 2007; Lennon et al., 2003; McNeil and Kirchhausen, 2005). Alternatively, an indirect role for dysferlin in wound repair may involve intercellular signaling (Chiu et al., 2009). For example, upon plasma membrane wounding a cell might release factors that signal other cells to compensate for the impairment or loss of the wounded cell.

To investigate the role of dysferlin in response to membrane wounding in an intact in vivo preparation, sea urchin embryos were used in conjunction with two-photon laser scanning microscopy to image Ca^{2+} signals before and after plasma membrane wounding.

Results

Laser wounding in conjunction with microscopy has been used to study how cells repair plasma membrane lesions (Bansal et al., 2003; Bi et al., 1995; McNeil et al., 2003). Studies in sea urchin eggs, fibroblasts, neurons and red blood cells using this approach revealed that plasma membrane repair requires extracellular Ca^{2+}, and fusion-competent internal membranes near the wound site (McNeil et al., 2003). In eggs, endomembranes rapidly respond to Ca^{2+} influx through the wound with local Ca^{2+}-triggered homo- and heterotypic fusion to seal and contain the breach at the wound site. The first issue addressed in this study was to determine if a rise in Ca^{2+} was restricted to the wounded cell, or if it also occurs in neighboring cells, a potential indicator of Ca^{2+}-triggered secretory events.

Membrane wounding evokes responses in neighboring cells

Fertilized sea urchin eggs (*Lytechinus variegatus*) were microinjected with the Ca^{2+} indicator Calcium Green-1 dextran (CGD), and then incubated at 24°C for approximately 2 hours until they reached the four-cell stage. Only embryos that successfully divided were used, to control for nonspecific injection damage. CGD-injected embryos were placed in artificial seawater (ASW) containing the membrane dye FM4-64 to observe plasma membrane wounding. FM4-64 is a red-shifted variant of FM1-43, and accordingly can be independently monitored in embryos stained with green fluorescent indicators (Covian-Nares et al., 2008). Embryos were imaged by time-lapse microscopy using two-photon laser scanning microscopy to simultaneously monitor CGD fluorescence, cell surface FM4-64 fluorescence, and DIC transmission images in all four blastomeres before and after one blastomere was wounded using a laser (Fig. 1A, and supplementary

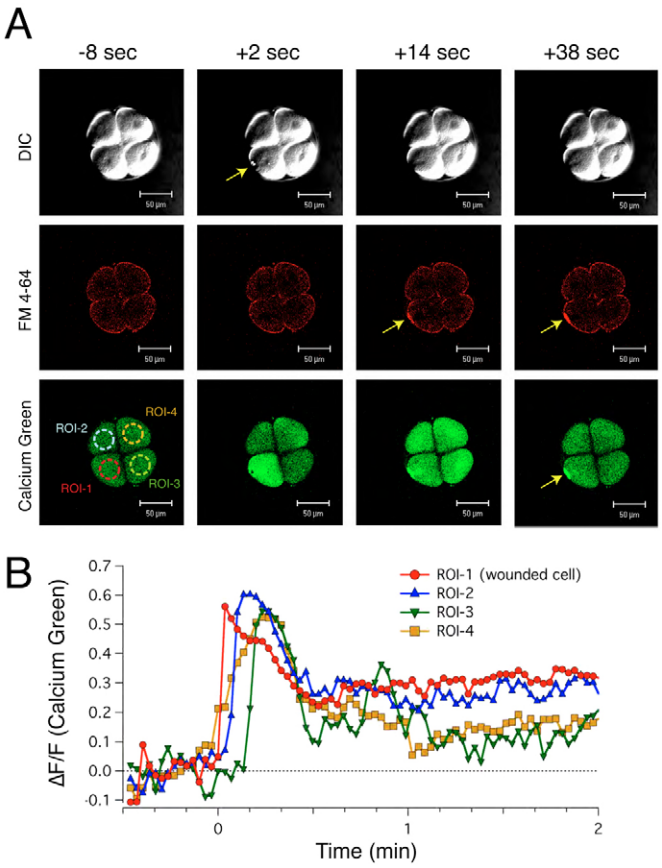

Fig. 1. Laser wounding triggers Ca^{2+} spikes in neighboring cells. (**A**) Differential interference contrast image (DIC, gray), FM 4-64 (red) and Calcium Green dextran (CGD) fluorescence (green) images of sea urchin embryos are shown 8 seconds prior to laser wounding (–8 sec), immediately after laser wounding a single blastomere (+2 sec), and at 14 (+14 sec) and 38 (+38 sec) seconds after laser wounding. Scale bars: 50 µm. (**B**) The timecourse of mean changes in CGD fluorescence (ΔF/F) are plotted for four ROIs (dashed red, blue, green and yellow regions in A): the blastomere wounded by the laser (red circles), two adjacent blastomeres that were not wounded (blue and green triangles), and the distal blastomere (yellow square).

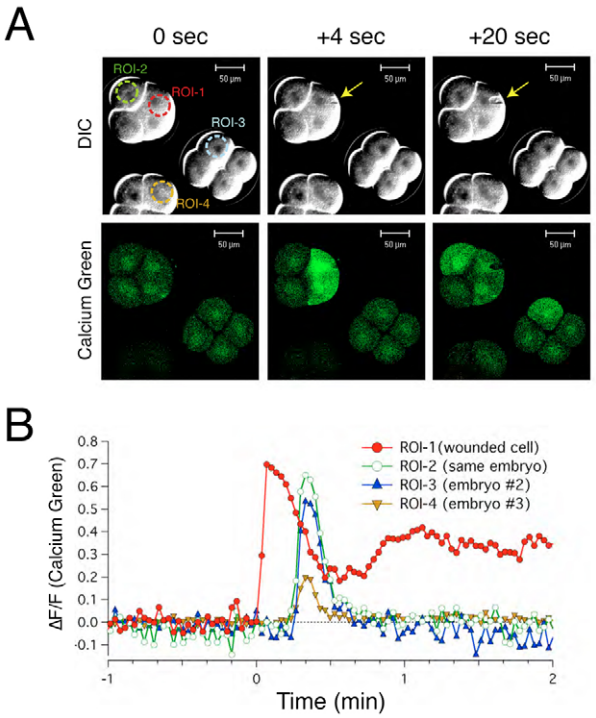

Fig. 2. Action at a distance. (**A**) Three non-contacting CGD-injected embryos were imaged by DIC and CGD two-photon microscopy immediately before (0 sec) and 4 (+4 sec) and 20 (+20 sec) seconds after laser wounding of a blastomere in one of the three embryos in the field (yellow arrow). (**B**) The timecourse of the CGD fluorescence change (ΔF/F) are plotted for four ROIs: the wounded blastomere (red circles), an adjacent blastomere in the wounded embryo (green open circles), and blastomeres in non-contacting embryos (blue and yellow triangles). ROIs 1-4 are demarcated on the DIC image in A by colored dashed circles.

material Movies 1, 2 and 3). DIC imaging revealed that other than the formation of a small transient 'bubble' visible in the first image acquired following laser wounding (yellow arrow, +2 seconds), no obvious change in cell morphology was observed. FM4-64 fluorescence was primarily observed in the plasma membrane compartment encompassing each blastomere, although some fluorescence was also observed in puncta throughout the embryo. By 14 seconds after wounding, a bright spot of FM4-64 fluorescence was observed at the cell surface of the laser-wounded cell (yellow arrows). The delayed formation of this scar suggests the focal and progressive addition of a reticulum of new membrane to the plasma membrane.

The intensity of CGD fluorescence was dramatically altered at the wound site (Fig. 2A, and supplementary material Movie 1). Immediately after wounding (+2 seconds) the injured blastomere displayed elevated Ca^{2+} concentrations. This rise in free Ca^{2+} was not limited to the wounding site, as CGD fluorescence intensity increased throughout the cytoplasm of the wounded cell. Surprisingly, with a short delay (typically 5-20 seconds) a rise in intracellular Ca^{2+} (i.e. a 'Ca^{2+} spike') was observed in cells neighboring the wounded blastomere. This rise in CGD fluorescence can be seen in the CGD image acquired at +14 seconds (Fig. 1A). A coordinated rise in CGD fluorescence was consistently observed in at least one of the three neighboring blastomere in 100% of the four-cell stage embryos tested (n=41). Also note that by +38 seconds after wounding the intensity of CGD fluorescence had declined globally in all four blastomeres except at the site of the wounding scab (yellow arrow). To better understand the dynamics of these Ca^{2+} spikes the mean intensity of four regions of interest (ROIs 1-4) were plotted as a function of time (Fig. 1B). Notice that the Ca^{2+} signal reached a maximal value in the wounded cell (ROI-1) by 2 seconds after wounding, while in the remaining three cells CGD fluorescence intensity peaked by 8 (ROI-2), 14 (ROI-4) and 16 (ROI-3) seconds after wounding. Also note that although these Ca^{2+} spikes had declined by 30 seconds after wounding, they did not returned to baseline values even after 2 minutes, indicating that plasma membrane wounding of one cell can cause both transient and persistent changes in the Ca^{2+} concentration of neighboring cells. Individual blastomeres of CGD-injected embryos that had not been laser wounded, or blastomeres prior to wounding occasionally displayed short spontaneous Ca^{2+} bursts (see the first 15 frames of supplementary material Movie 1 prior to laser wounding, or black arrows in Fig. 3A). These 'spontaneous' Ca^{2+} bursts did not appear

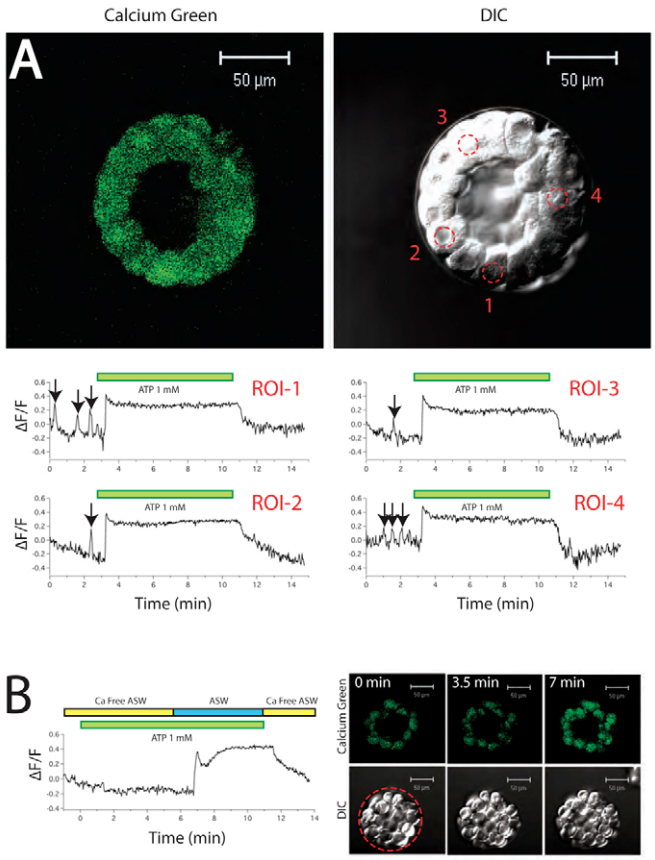

Fig. 3. Extracellular ATP triggers Ca^{2+} spikes in sea urchin embryos. (**A**) A CGD-injected embryo at the blastula stage was perfused with ASW supplemented with 1 mM ATP and imaged by time-lapse DIC and two-photon fluorescence microscopy. The timecourse of CGD fluorescence (ΔF/F) is plotted for four ROIs in four individual blastomeres in the same embryo. These ROIs are demarcated on the DIC image in A by red dashed circles. Green bars indicate the duration of ATP perfusion. Note the spontaneous non-synchronized Ca^{2+} spike activity observed in individual blastomeres prior to ATP perfusion (black arrows). (**B**) In Ca^{2+}-free ASW (yellow bar) ATP perfusion (green bar) failed to trigger a rise in intracellular Ca^{2+} as measured by CGD fluorescence. Returning the embryo to ASW with normal Ca^{2+} (~9 mM; blue bar) restored the embryo's ability to respond to ATP perfusion. Note that in Ca^{2+}-free ASW sea urchin tight junctions are destabilized with individual blastomeres assuming a rounded appearance in the DIC image. This rounded morphology did not immediately reverse upon perfusion with normal ASW. Despite this change in cell morphology, extracellular ATP could trigger intracellular Ca^{2+} spikes as long as extracellular Ca^{2+} was present.

to be coordinated with any specific event or between individual blastomeres.

Plasma membrane wounding could potentially generate Ca^{2+} spikes in neighboring cells by two signaling mechanisms. Wounding might cause the release of signaling factors into the extracellular milieu. Eventually these released factors evoke Ca^{2+} spikes in neighboring cells. Alternatively, a wounded cell and its neighbors might be coupled structurally (e.g. through gap junctions). In this type of mechanism the release of a soluble signaling factor is not required. If plasma membrane wounding triggered the release of a soluble factor, the wounding of a blastomere in one embryo might trigger a Ca^{2+} spike in a nearby but non-contacting embryo. Groups of adjacent embryos were microinjected with CGD and allowed to develop. Fig. 2A (supplementary material Movie 4) shows a field with three CGD-injected embryos that are adjacent, but non-contacting. A blastomere in the upper-left embryo was laser wounded (yellow arrow) which immediately evoked a Ca^{2+} spike in the wounded cell (Fig. 2B, ROI-1). Sixteen seconds later Ca^{2+} spikes were observed in a neighboring cell in the same embryo (ROI-2), as well as in cells of two other non-contacting embryos (ROIs 3 and 4). The ability of laser wounding to trigger Ca^{2+} spikes at a distance was observed in 25 out of 30 similar experiments [fraction, *f*, equals 0.83, with a 95% confidence interval ($CI_{95\%}$) of 0.66–0.93], suggesting that laser wounding results in the release of a signaling factor.

The signaling factor is an apyrase substrate

One candidate for the signaling factor released from laser-wounded cells is ATP. ATP efflux is used for both paracrine and autocrine signaling, primarily by binding to cell surface purinergic receptors (Burnstock, 2006). Perfusion of embryos microinjected with CGD with seawater containing ATP resulted in a coordinated sustained rise in fluorescence in virtually every cell in the embryo (Fig. 3A). The CGD fluorescence intensity returned to baseline values when extracellular ATP was removed. A similar response was observed in 19 out of 22 embryos tested (*f*=0.86, $CI_{95\%}$ 0.66-0.96). By contrast, transient non-coordinated Ca^{2+} bursts (as previously mentioned) were observed in some blastomeres prior to exposure to ATP (Fig. 3A, black arrows). A rise in intracellular Ca^{2+} in response to perfusion with ATP was only observed when embryos were in seawater containing Ca^{2+} (Fig. 3B), suggesting that Ca^{2+} influx, probably through a P2X type receptor, is required for the ATP response.

The magnitude of the average CGD fluorescence change observed with ATP perfusion was similar in magnitude to the change observed with laser wounding in individual cells (compare Fig. 4A and Fig. 1B). Perfusion with ADP evoked a similar response (Fig. 4B; observed in 13 out of 15 embryos, *f*=0.87 with a $CI_{95\%}$ of 0.62-0.92), but perfusion with AMP always failed to evoke a rise in intracellular Ca^{2+} (Fig. 4C; *n*=15 embryos, *f*=0 with a $CI_{95\%}$ of 0 to 0.24).

Apyrase, is an enzyme that degrades ATP and ADP to AMP (Boyd and Forrester, 1968). If laser wounding triggers the release of ATP from the wounded cell, addition of extracellular apyrase to the seawater should attenuate the Ca^{2+} spikes in neighboring cells caused by laser wounding. This was observed when 20 units/ml of apyrase was added to the seawater (Fig. 4D and supplementary material Movies 5 and 6; seen in 21 out of 26 embryos, *f*=0.81 with a $CI_{95\%}$ of 0.62 to 0.92).

Voltage-gated Ca^{2+} channels are required for wound triggered signaling

One pathway for the release of a soluble signaling factor, such as ATP, from wounded cells is by diffusion through the wound itself, although other release mechanism are possible (Anselmi et al., 2008). For example, in excitable cells, such as echinoderm eggs (Jaffe and Robinson, 1978), wounding transiently depolarizes their membrane potential (Fein and Terasaki, 2005). In many cells, depolarization opens voltage-gated Ca^{2+} channels (VGCC), and Ca^{2+} influx through these channels can trigger exocytosis. As ATP is known to be stored in the lumen of many secretory vesicles, it is possible that wounding might trigger exocytotic release of ATP (Douglas and Poisner, 1966; Morel and Meunier, 1981; Pangrsic et al., 2007). To evaluate if a depolarization mechanism involving

Ca^{2+} channels is operant, we tested if cadmium, a divalent cation that blocks most VGCCs, can interfere with wound-stimulated Ca^{2+} spikes in neighboring cells. Addition of $CdCl_2$ was found to block Ca^{2+} spikes in neighboring cells (Fig. 5A), and was effective in all embryos tested (n=25, f=1 with a $CI_{95\%}$ of 0.84-1). Wounding in seawater containing either nifedipine (n=31), a specific inhibitor of L-type VGCC, or ω-conotoxin GVIA (n=15), a specific inhibitor of N-type VGCC did not block intercellular signaling (Fig. 5B and C, respectively). Like $CdCl_2$, ω-agatoxin IVA, a specific inhibitor of the P/Q-type VGCC also blocked Ca^{2+} spikes in neighboring cells (Fig. 5D). Inhibition with agatoxin was observed in 19 out of 24 embryos tested (f=0.79 with a $CI_{95\%}$ of 0.59-0.91), suggesting that agatoxin-sensitive channels play an important role in this intercellular signaling mechanism.

If VGCCs mediate the release of ATP following wounding, membrane depolarization should trigger ATP release. A firefly luciferase-based luminescence assay was used to directly measure ATP release from sea urchin embryos. Luminescence catalyzed by firefly luciferase is specific for ATP. Washed embryos were incubated for 1 minute in either ASW, ASW containing KCl (to depolarize their membrane potential), or ASW with both KCl and cadmium (to block VGCCs). Following incubation, the isolated supernatant from these samples were assayed for ATP using a firefly luciferase luminescence assay (Fig. 5E). KCl depolarization resulted in a 3.7-fold increase in luminescence compared with an ASW control, and the addition of cadmium blocked ATP secretion in response to depolarization. ANOVA indicated that the release of ATP with KCl compared with the control (P<0.001) or in the presence of cadmium (P<0.001) was significant. Thus, it is likely that VGCCs open when membranes are wounded, which triggers ATP secretion. Although it is possible that agatoxin might also block the ability of cells to respond to secreted ATP, this seems unlikely because agatoxin was found to block Ca^{2+} spikes in neighboring cells, but did not block the ability of these cells to respond to ATP application (Fig. 5F and supplementary material Movies 7 and 8).

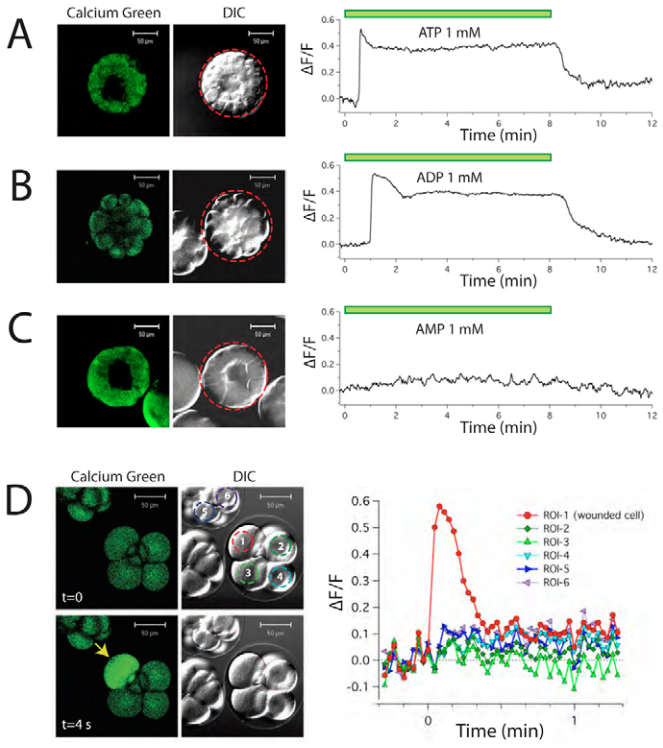

Fig. 4. Apyrase blocks the intercellular signaling triggered by laser wounding. CGD-injected embryo at the blastula stage was perfused with ASW supplemented with 1 mM ATP (**A**), ADP (**B**), or AMP (**C**) and imaged by time-lapse DIC and fluorescence microscopy. The timecourse of CGD fluorescence (ΔF/F) is plotted for ROIs encompassing the whole embryo, and are demarcated on the respective DIC image by red dashed circles. Green bars indicate the duration of nucleotide perfusion. (**D**) When a blastomere of a CGD-injected embryo was wounded with a laser (yellow arrow) in ASW supplemented with apyrase (20 IU/ml), Ca^{2+} spikes in adjacent blastomeres and in neighboring embryos were no longer observed.

Antisense dysferlin morpholino oligonucleotide inhibits wound-triggered signaling

A loss-of-function strategy was adopted to investigate whether dysferlin is involved in intercellular signaling in response to wounding. Sequence-specific phosphorodiamidate morpholino oligonucleotides (morpholinos) have been successfully used in developing sea urchin embryos to knock-down the expression of specific genes by inhibiting RNA translation or splicing (Angerer and Angerer, 2004). The 5′ untranslated region, translation start site, and coding regions from exons 1 and 2 of sea urchin dysferlin were cloned and sequenced (supplementary material Fig. S1A-C). RT-PCR was then used to demonstrate that mRNA encoding sea urchin dysferlin is present in *L. variegatus* eggs (supplementary material Fig. S1D).

To test if dysferlin is involved in the signaling pathway that triggers Ca^{2+} spikes in neighboring cells, embryos were co-injected at the one-cell stage with CGD and either antisense or sense sea urchin dysferlin morpholinos based on the sequence spanning sea urchin dysferlin exons 1 and 2. Only embryos that successfully underwent at least two rounds of cell division were used to control for nonspecific injection damage, and to account for protein turnover. Individual blastomeres were wounded and Ca^{2+} spikes were monitored in the wounded and in neighboring non-wounded blastomeres. Representative fluorescence and DIC images of embryos co-injected with CGD and antisense dysferlin morpholino are shown in Fig. 6A (see also supplementary material Movies 9 and 10). The normalized CGD fluorescence intensity (ΔF/F) of ROIs representing the wounded blastomere (ROI-1), non-wounded cells in the same embryo (ROI-2), and cells in neighboring embryos (ROIs 3-5) are plotted as a function of time after laser wounding. A rise in Ca^{2+} was only observed in the wounded cell. Complete inhibition of wound-correlated Ca^{2+} spike activity in neighboring cells was observed in 71.7% of embryos injected with the antisense dysferlin morpholino (Ca^{2+} spikes in neighboring cells were observed in only 13 out of 46 embryos, f=0.28 with a $CI_{95\%}$ of 0.17-0.43) suggesting that dysferlin is involved in this wound-triggered intercellular signaling pathway. As a control for non-specific morpholino inhibition, the sense dysferlin morpholino was injected into sea urchin embryos. Fig. 6B shows representative images of embryos co-injected with CGD and the sense dysferlin morpholino. Ca^{2+} spikes in the wounded cell as well as in neighboring cells (with a short delay) were observed in ROI CGD fluorescence traces. Ca^{2+} spikes were seen in at least one non-wounded neighboring cell in 15 out of 16 embryos microinjected with the sense dysferlin morpholino (f=0.94 with a $CI_{95\%}$ of 0.70-0.99). Fisher's analysis indicates a statistically significant difference between antisense and sense morpholino injection (P<0.0001 using

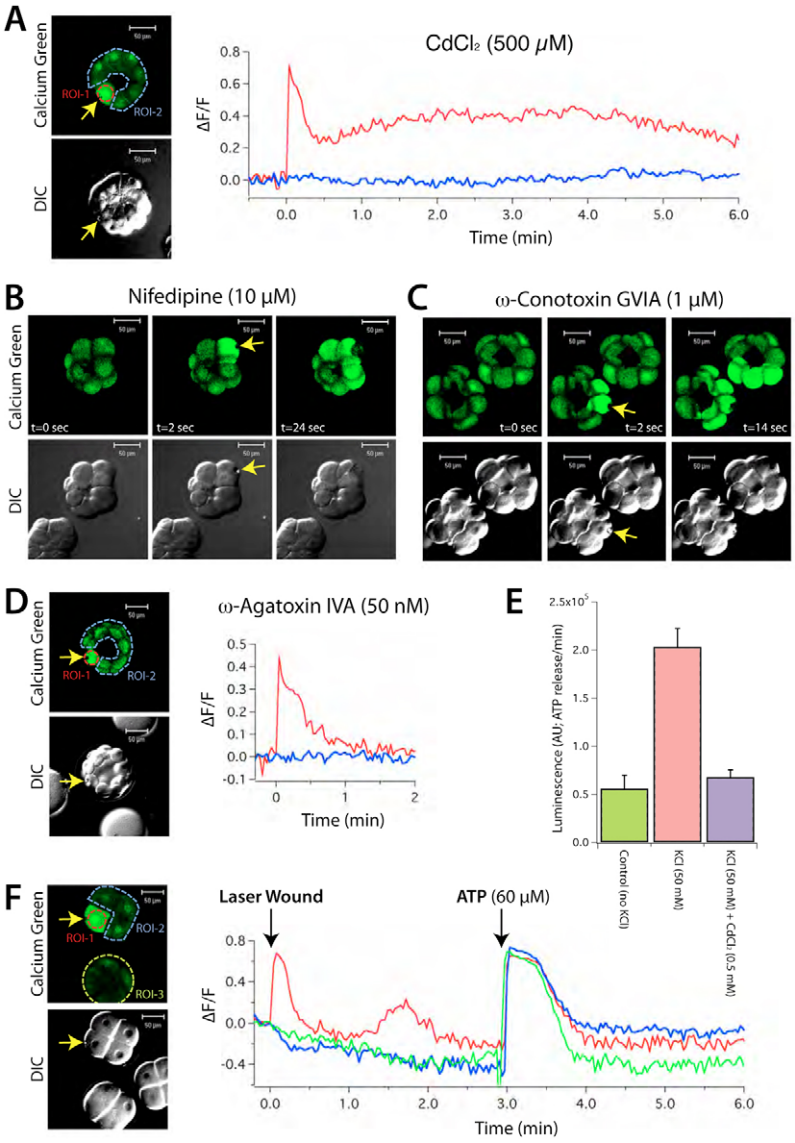

Fig. 5. Voltage-gated Ca^{2+} channels mediate the intercellular signaling triggered by wounding. A blastomere of a CGD-injected embryo was laser wounded (yellow arrow) in ASW supplemented with 500 μM $CdCl_2$ (**A**), 10 μM nifedipine (**B**), 1 μM ω-conotoxin GVIA (**C**), or 50 nM ω-agatoxin IVA (**D**). (**E**) Depolarization of sea urchin embryos with 50 mM KCl triggered the release of ATP as measured using a firefly luciferase luminescence assay (compare green and red bars). ATP secretion in response to high KCl was blocked by 500 μM $CdCl_2$ (blue bar). All points are mean ± s.d. n=19. (**F**) A blastomere of a CGD-injected embryo was laser wounded (yellow arrow) in ASW supplemented with 50 nM ω-agatoxin IVA. Three minutes after laser wounding, ATP (60 μM) was added to the bath and evoked Ca^{2+} spikes in the previously wounded blastomere (ROI-1, red line), in adjacent blastomeres in the same embryo (ROI-2, blue line), as well as in blastomeres in another CGD-injected embryo (ROI-3, green line).

a 2×2 contingency table). As an additional control against non-specific morpholino effects, 25-base mixed oligonucleotides having a random base mixture at every position (random morpholino) were injected into sea urchin embryos. Microinjection of the random morpholino also failed to block Ca^{2+} spikes in neighboring cells (Fig. 6C). This was observed in all embryos injected with the random morpholino (n=20, f=1 with a $CI_{95\%}$ of 0.83-1).

The inhibition of intercellular signaling that was observed with the antisense dysferlin morpholino could potentially arise by inhibition of the release of a signaling factor. Alternatively, it might prevent signaling by blocking the ability of neighboring cells to respond. Based on the observation that ATP application stimulates Ca^{2+} spikes in sea urchin, that depolarized sea urchin eggs release ATP, and that extracellular apyrase blocks intercellular signaling, it seems plausible that ATP is the signaling factor released by wounded cells. To discern the signaling step that morpholinos perturb, embryos were co-injected with the antisense dysferlin morpholino and CGD. After several rounds of cell division these embryos were perfused with ATP while monitoring CGD fluorescence. A sustained rise in fluorescence was observed upon perfusion with ATP (Fig. 6D) in every embryo injected with the antisense dysferlin morpholino (n=20). Accordingly, if ATP is the signaling factor, it is likely that dysferlin mediates the release of ATP rather than the cellular response to ATP application. Although we have shown that depolarized embryos release ATP, the substrate specificity of apyrase for nucleotide tri- and diphosphates does not preclude the possibility that other nucleotides may be co-released with wounding.

Presumably the microinjection of antisense morpholinos reduces the expression of dysferlin. Attempts were made to produce an antibody to directly monitor the abundance of sea urchin dysferlin but unfortunately these attempts failed to produce a specific antiserum. We also tested a polyclonal antibody with specificity for human dysferlin (Abcam Inc.; ab52242), but this reagent failed to cross-react with sea urchin dysferlin. Accordingly, an alternative strategy for testing the specificity of the antisense dysferlin morpholino based on rescuing the observed loss-of-function was adopted. Because the sea urchin antisense dysferlin morpholino has no homology with human dysferlin, if human dysferlin performs a similar function as sea urchin dysferlin, co-injection of mRNA

encoding human dysferlin along with the sea urchin antisense dysferlin morpholino might rescue wound-triggered intercellular signaling.

Co-injection of mRNA encoding human dysferlin rescues wound-triggered intercellular signaling

The human dysferlin gene is large (~6200 bp), thus, before attempting to use mRNA encoding human dysferlin to rescue the loss-of-function it was important to confirm that intact mRNA capable of expressing membrane bound dysferlin could be isolated. Dysferlin is a tail-anchored integral membrane protein with the bulk of its mass residing in the cytoplasm. Only a short C-terminal segment of the protein distal to its single membrane-spanning domain resides outside of the cell. Two plasmids encoding human dysferlin were prepared for generating mRNA; one (dysferlin-Venus) in which Venus (Nagai et al., 2002) (a yellow spectral variant of green fluorescent protein) was placed at the C-termini, and a second (dysferlin-3HA) with a much shorter optimized hemagglutinin tag attached to the C-termini. HeLa cells were electroporated with these mRNAs and the next day live cells were incubated with an Alexa Fluor 594 HA-domain-specific antibody conjugate, and imaged by wide-field fluorescence microscopy (using filter sets specific for either Venus or Alexa Fluor 594; supplementary material Fig. S2A). The spatial distribution of dysferlin-Venus fluorescence was noticeably similar to Alexa Fluor 594 fluorescence, which was primarily membrane localized. Cells transfected with a mixture of these mRNAs revealed one subtle difference between the spatial distributions of Venus and Alexa Fluor 594 fluorescence. Venus fluorescence was observed in a perinuclear compartment, most likely the Golgi complex, whereas Alexa Fluor fluorescence was absent in this region (supplementary material Fig. S2B, white arrows). Thus, dysferlin-3HA is expressed on the cell surface when mRNA encoding this construct is introduced into cells.

To test whether mRNA encoding human dysferlin can rescue the loss-of-function caused by the antisense sea-urchin-specific morpholino, embryos were co-injected with CGD and the antisense dysferlin morpholino (Fig. 6A), or with CGD, the antisense

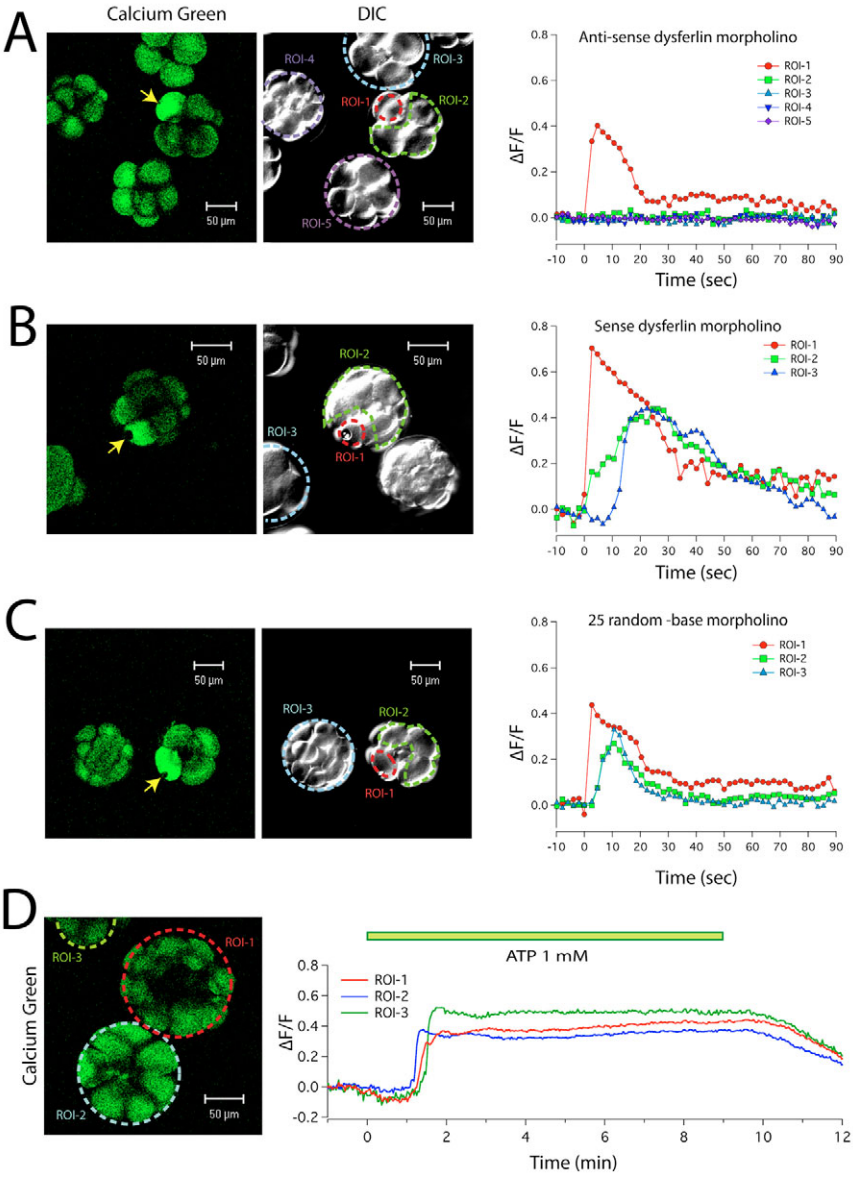

Fig. 6. Antisense dysferlin morpholinos inhibit intercellular signaling triggered by laser wounding. Sea urchin embryos were injected at the one-cell stage with CGD (5 mg/ml) and 1 mM antisense dysferlin morpholino (**A**), sense dysferlin morpholino (**B**), or a 25 random-base negative control morpholino (**C**). Following a 3-hour incubation period the embryos were imaged by time-lapse DIC and two-photon fluorescence microscopy before and after laser wounding a single blastomere (yellow arrow). The timecourse of mean CGD fluorescence changes (ΔF/F) is plotted for ROIs in the laser wounded blastomere (ROI-1, demarcated on the respective DIC image by red dashed circles; red symbols), blastomeres adjacent to the laser wounded blastomere (ROI-2, demarcated on the respective DIC image by a green dashed line; green symbols), and blastomeres in nearby non-contacting embryos. (ROIs 3-5, demarcated on the respective DIC image by blue and purple dashed lines, and correspondingly colored symbols). (**D**) Sea urchin embryos were injected at the one-cell stage with CGD and the antisense dysferlin morpholino. Injected embryos at the blastula stage were perfused with ASW supplemented with 1 mM ATP and imaged by time-lapse two-photon CGD fluorescence imaging. The timecourse of mean CGD fluorescence changes (ΔF/F) is plotted for three ROIs in the three different embryos. All three embryos responded to perfusion with ATP (green bar) with a rise in CGD fluorescence despite being injected with antisense dysferlin morpholino.

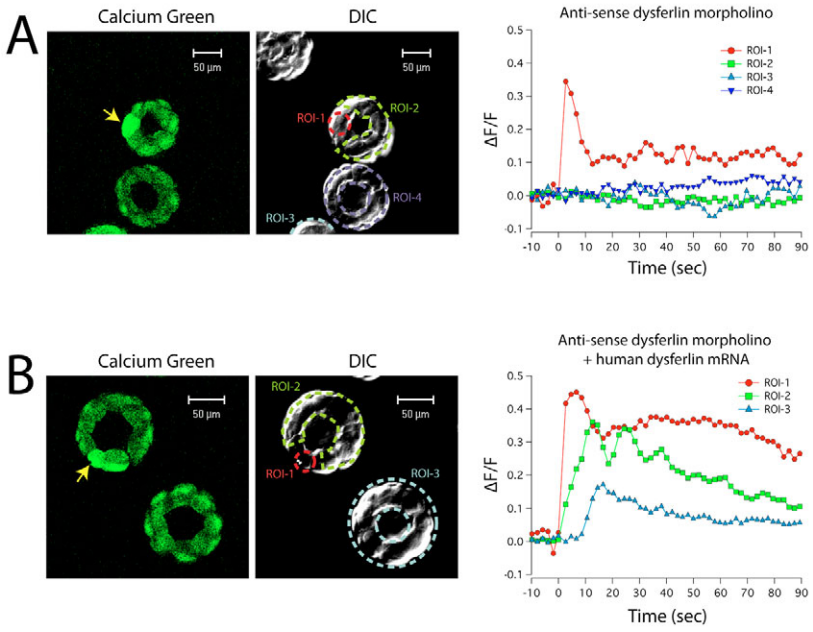

Fig. 7. Co-injection of mRNA encoding human dysferlin rescues antisense dysferlin morpholino inhibition. (**A**) Sea urchin embryos were injected at the one-cell stage with CGD and the antisense dysferlin morpholino. Following a 3-hour incubation period the embryos were imaged by time-lapse DIC and two-photon fluorescence microscopy before and after laser wounding of a single blastomere (yellow arrow). The timecourse of mean CGD fluorescence changes (ΔF/F) is plotted for ROIs in the laser-wounded blastomere (ROI-1, demarcated on the respective DIC image by a red dashed line; red symbols), blastomeres adjacent to the laser-wounded blastomere (ROI-2, demarcated on the respective DIC image by green dashed line; green symbols), and blastomeres in nearby non-contacting embryos. (ROI-3 and 4, demarcated on the DIC image by blue and purple dashed lines, and correspondingly colored symbols). (**B**) Sea urchin embryos were injected at the one-cell stage with CGD, the antisense dysferlin morpholino, and mRNA encoding the 3HA-tagged human dysferlin. Following a 3-hour incubation period the embryos were imaged by time-lapse DIC and two-photon fluorescence microscopy before and after laser wounding of a single blastomere (yellow arrow). The timecourse of mean CGD fluorescence changes (ΔF/F) is plotted for ROIs in the laser-wounded blastomere (ROI-1, demarcated on the respective DIC image by red dashed lines; red symbols), blastomeres adjacent to the laser wounded blastomere (ROI-2, demarcated on the respective DIC image by a green dashed line; green symbols), and blastomeres in a nearby non-contacting embryo. (ROI-3, demarcated on the DIC image by a blue dashed line; blue symbols.)

dysferlin morpholino and mRNA encoding the 3HA-tagged human dysferlin (0.24 μg/μl; approximately 110 nM assuming a 200 base poly(A) tail). As observed previously, microinjection of the antisense morpholino blocked the intercellular signaling triggered by cell wounding (Fig. 7A, and supplementary material Movies 11 and 12). Complete inhibition of wound-correlated Ca^{2+} spike activity in neighboring cells was observed in 76.9% of embryos injected with the antisense dysferlin morpholino (Ca^{2+} spikes in neighbors were observed in three out of 13 trials, f=0.23 with a $CI_{95\%}$ of 0.08-0.51). By contrast, Ca^{2+} spikes were observed in neighboring cells when mRNA encoding dysferlin-3HA was co-injected with the antisense morpholino (Fig. 7B, and supplementary material Movies 13 and 14). The human dysferlin mRNA rescue of intercellular signaling activity was observed in all co-injected embryos (n=11, f=1 with a $CI_{95\%}$ of 0.70-1.0). Fisher's analysis indicates a statistically significant difference with human dysferlin mRNA co-injection (P<0.0002).

Discussion

While monitoring changes in intracellular Ca^{2+} concentration in developing embryos, Ca^{2+} spikes were observed in laser-wounded cells, and following a short delay spikes were also seen in neighboring cells that had not been directly injured (Fig. 1). In osteoblastic cells Ca^{2+} spikes similar to these are mediated by gap-junctional communication between adjoining cells (Jorgensen et al., 2000). Such a mechanism cannot completely explain the signaling observed in sea urchin because delayed Ca^{2+} spikes were observed in non-contacting embryos (Fig. 2). Gap-junctional communication, while possible, seems unlikely as genes encoding connexins, pannexins and innexins, the proteins that form gap-junctions and hemichannels, are not found in the sea urchin genome (Sodergren et al., 2006). We conclude that plasma membrane wounding in developing sea urchin embryos initiates a mechanism that releases a water-soluble signaling factor that can evoke Ca^{2+} spikes in neighboring cells. This conclusion was further supported by the observation that perfusion with seawater containing ATP or ADP but not AMP also triggered a rise in intracellular Ca^{2+} (Figs 3 and 4). When embryos were placed in seawater containing apyrase, laser-induced damage failed to evoke Ca^{2+} spikes in neighboring cells (Fig. 4D) indicating that the factor released from wounded cells is most likely ATP, or a related nucleotide tri- or diphosphate. Incubation in seawater containing apyrase did not appear to inhibit wound repair as judged by DIC imaging of the wounded blastomere, and by the near complete recovery of the CGD signal in the wounded cell (Fig. 4D, and see discussion below), suggesting that in sea urchin embryos the action of released nucleotides is not required for membrane resealing.

When embryos were placed in seawater containing agatoxin or cadmium, two inhibitors of P/Q-type VGCCs, laser wounding no longer evoked Ca^{2+} spikes in neighboring cells (Fig. 5), whereas Ca^{2+} spikes were observed with inhibitors of N-type and L-type channels. These experiments suggest that Ca^{2+} influx, specifically through an agatoxin-sensitive Ca^{2+} channel, is required for the injury-evoked release of nucleotides. In fertilized sea urchin eggs

Ca^{2+} influx through agatoxin-sensitive VGCCs is known to trigger compensatory endocytosis (Covian-Nares et al., 2008; Smith et al., 2000; Vogel et al., 1999), and agatoxin-sensitive channels have been shown to be translocated to the cell surface immediately after fertilization (Smith et al., 2000). As plasma membrane wounding is known to cause depolarization of embryos (Fein and Terasaki, 2005), we speculate that these same VGCCs would be available to mediate Ca^{2+} influx and the subsequent release of nucleotides. Consistent with this hypothesis, we showed directly that ATP is released from sea urchin embryos when they were depolarized using high KCl (Fig. 5E), and that ATP release was blocked by cadmium. Although plasma membrane wounding in seawater containing agatoxin failed to evoke Ca^{2+} spikes in neighboring cells, agatoxin did not prevent a rise in Ca^{2+} in response to applied ATP (Fig. 5F). Thus, ATP-evoked Ca^{2+} spikes must not require Ca^{2+} influx through agatoxin-sensitive channels.

Plasma membrane wounding in seawater containing either $CdCl_2$ or agatoxin did not prevent a global rise in Ca^{2+} concentration throughout the damaged cell (Fig. 5A,D,F). Clearly, Ca^{2+} could still enter the wounded cell through the lesion, and potentially activate many intracellular signaling pathways (Whitaker, 2006). As agatoxin did not appear to inhibit wound repair, as judged by DIC imaging of the wounded blastomere that showed near complete recovery of the CGD signal in the wounded cell, and by the ability of the wounded cell to respond to the subsequent application of ATP (Fig. 5F), it seems likely that Ca^{2+} influx through the wound itself is sufficient for wound repair, while Ca^{2+} influx through agatoxin-sensitive VGCCs is required for intercellular signaling. These experiments also suggest that the Ca^{2+}-activated machinery required for intercellular signaling resides in close proximity to the pores of agatoxin-sensitive channels and requires high concentrations of Ca^{2+} for activation. Interestingly otoferlin, a dysferlin homolog involved in neurotransmitter release in the inner ear (Roux et al., 2006) binds to L-type VGCCs (Ramakrishnan et al., 2009).

It is worth considering four possible mechanisms for the release of nucleotides in response to plasma membrane wounding: (1) nucleotides diffuse out of the cell through the wound itself; (2) wounding causes depolarization initiating Ca^{2+} influx through VGCCs, which triggers exocytotic secretion; (3) wounding and the subsequent depolarization (or Ca^{2+} spike) opens channels on the cell surface, such as hemichannels, allowing the diffusion of nucleotides through these channels; and (4) wounding activates pumps on the cell surface that transport these nucleotides from the cytoplasm to the extracellular milieu. The $CdCl_2$ and agatoxin sensitivity of intercellular signaling seemingly eliminates mechanism 1 from further consideration, as nucleotide diffusion through a plasma membrane wound should not be impeded by these channel blockers. It is also unlikely that nucleotides were released from wounded cells through hemichannels because genes encoding the proteins that are known to form hemichannels, are not found in the sea urchin genome (Sodergren et al., 2006). Although agatoxin-sensitive channels or pumps that can directly transport nucleotides have not been reported, we cannot rule out the possibility that they may exist and are responsible for nucleotide release following wounding as postulated in the third and fourth proposed mechanisms. Nonetheless, the most likely explanation for how agatoxin blocks intercellular signaling is that it inhibits the gating of P/Q-type Ca^{2+} channels as outlined in mechanism 2.

RT-PCR indicated that sea urchin eggs have mRNA encoding dysferlin (supplementary material Fig. S1D). Microinjection of an antisense dysferlin morpholino into developing embryos blocked the intercellular signaling pathway activated by laser wounding (Fig. 6A and Fig. 7A). Sense and random control morpholinos did not block this signaling pathway (Fig. 6B,C). Thus, we conclude that the observed morpholino-evoked loss-of-function is specific for the complementary nucleotide sequence of the antisense dysferlin morpholino. This sequence specificity was confirmed by rescuing the morpholino-induced loss-of-function by co-injecting mRNA encoding human dysferlin (Fig. 7B). As the antisense dysferlin morpholino has no homology with human dysferlin (as determined by BLAST analysis; http://blast.ncbi.nlm.nih.gov/Blast.cgi) the human dysferlin mRNA rescue of morpholino-induced loss-of-function suggests that dysferlin in humans has the same or a similar function as in sea urchin.

The antisense dysferlin morpholino blocked intercellular signaling (Fig. 6A and Fig. 7A), but did not prevent a Ca^{2+} spike in the wounded cell, or the ability of applied ATP to evoke Ca^{2+} spikes (Fig. 6D). If the soluble signaling factor is ATP, these experiments suggest that dysferlin mediates a step in this signaling cascade that is upstream of the release of ATP from the wounded cell. In *C. elegans* Fer-1, a dysferlin homolog, is thought to mediate the Ca^{2+}-triggered exocytotic fusion of vesicles involved in sperm activation (Washington and Ward, 2006). Similarly, otoferlin, another dysferlin homolog found in cochlear hair cells is thought to mediate the Ca^{2+}-triggered exocytotic release of neurotransmitters (Roux et al., 2006). Thus, by analogy with Fer-1 and otoferlin, and considering that dysferlin has multiple Ca^{2+} binding domains, we propose that dysferlin mediates or regulates a step between Ca^{2+} influx and the Ca^{2+}-triggered release of a signaling factor. Although it is tempting to speculate that dysferlin mediates exocytosis, this has not been demonstrated by our experiments, and we cannot rule out the possibility that dysferlin might mediate some other critical step required for nucleotide release.

DIC imaging revealed that cells from embryos injected with the antisense dysferlin morpholino remained intact, even after laser wounding (see supplementary material Movies 9 and 11), and appeared similar to DIC images of wounded control cells that had not been injected (supplementary material Movie 3). This response was dramatically different from sea urchin eggs and fibroblasts that rapidly lyse in response to laser wounding in Ca^{2+}-free buffers (conditions that blocked membrane repair) (McNeil et al., 2003) and suggest that in sea urchin dysferlin is not required to repair wounded membrane. This conclusion was also reached by analyzing CGD intensity traces before and after laser wounding. Laser wounding typically evoked a transient rise in CGD fluorescence in wounded cells, and by 30 seconds after wounding fluorescence usually decayed to a steady state intensity that was higher than the initial baseline values (Figs 1, 2, 4-7). This was observed with normal embryos, with embryos injected with either antisense or sense dysferlin morpholinos, or with random morpholinos. The intensity of CGD fluorescence should be a function of the dye concentration, as well as of the free Ca^{2+} concentration inside the cell. Although a rise in fluorescence indicates an increase in free Ca^{2+} concentration, the subsequent decay of fluorescence might represent a loss of indicator from the wounded cell rather than a decrease in Ca^{2+} concentration. Several lines of reasoning suggest that the decay of CGD fluorescence primarily represents a decrease in free Ca^{2+}. First, sea urchin eggs are known to rapidly repair plasma membrane wounds (Miyake and McNeil, 1995), and we have verified this using FM4-64 imaging (Fig. 1). Second, the duration of a Ca^{2+} spike, typically 20 seconds, was similar in

wounded and neighboring non-wounded cells (Fig. 1). Third, as mentioned above, after wounding, CGD fluorescence intensity did not decay to values that were less than the baseline values prior to wounding, and typically decayed to values that were above this value. We do not understand the significance of this increase above baseline fluorescence, but it does indicate that at least some CGD must remain in these cells long after wounding had occurred. Based on both DIC and CGD imaging we conclude that in sea urchin embryos the microinjection of antisense dysferlin morpholino did not noticeably interfere with wound repair.

The absence of any obvious effects on wound repair using antisense dysferlin morpholinos is quite different from the results of experiments conducted using vertebrate muscle fibers isolated from dysferlin-null mice (Bansal et al., 2003). In those experiments the absence of dysferlin correlated with a dramatic decrease in the ability of muscle fibers to repair laser-induced membrane wounds. This discrepancy might reflect differences in the function of dysferlin in these two systems. As sea urchin is a member of the phylum Echinodermata, with members found in the fossil record dating back ~450 million years, it is possible that the role of dysferlin in mediating nucleotide release is a primordial function of the protein. Its role in muscle membrane repair may be a subsequent evolutionary adaptation. Alternatively, the discrepancy might reflect a difference between acute perturbations that presumably only partially reduced the expression of endogenous dysferlin (using morpholinos) and chronic perturbations where dysferlin expression was completely eliminated in knockout mice. Finally, the absence of any obvious effects on wound repair might reflect a difference between the in vivo function of dysferlin in intact developing embryos and its role in isolated muscle fibers.

It is tempting to speculate that in healthy humans, in addition to its role in membrane resealing, dysferlin might also mediate the release of ATP from muscle in response to wounding or exercise. Although this remains to be demonstrated, if dysferlin does mediate wounding-evoked intercellular signaling, a puzzling aspect of LGMD2B and MMD might be explained. Autosomal recessive mutations in a gene encoding a protein required for membrane repair are expected to be lethal, or minimally manifest early in development. Surprisingly, the progressive muscle weakness and deterioration associated with LGMD2B and MMD are normally not observed in children, rather these symptoms are typically observed in young adult. In children, muscle mass progressively increases through adolescence (Neu et al., 2002). In adults, muscle mass declines with aging, but this loss can be assuaged with exercise (Koopman and van Loon, 2009). If a function of dysferlin is to regulate the maintenance of muscle mass in adults via intercellular signaling, the symptoms of dysferlinopathies would be expected to manifest in young adults when the maintenance of muscle mass switches to a feedback mechanism driven by exercise and its associated muscle wounding.

In developing embryos we have documented a new intercellular signaling pathway, initiated by plasma membrane insult, that involves the Ca^{2+}-dependent release of ATP from wounded cells. Nucleotide release can then trigger Ca^{2+} spikes in neighboring cells. Our experiments indicate that in sea urchin, antisense dysferlin morpholinos can block intercellular signaling, presumably by preventing the release of ATP, and that this inhibition occurs under conditions in which direct wound repair is not detectibly altered. Although it is well known that intracellular Ca^{2+} can modulate many cellular functions, the target of this signaling pathway is not known. We speculate that the purpose of this pathway is to coordinate activities in different blastomeres during early development. It is also not known if the components mediating this pathway are recruited specifically to respond to wounding, or if membrane depolarization commandeers their activities from some other purpose. A better understanding of the heretofore overlooked role of trauma-induced nucleotide release as well as the mechanism through which it operates may reveal new details of early development, and suggest therapeutic approaches for the management of LGMD2B and MMD.

Materials and Methods

Reagents

Reagents were purchased from Invitrogen Inc. (Carlsbad, CA) unless otherwise specified. Restriction endonucleases were obtained from New England Biolabs, and the SMART RACE cDNA Amplification Kit was purchased from Clonetech (Mountain View, CA). Oligonucleotides were designed using MacVector (Cary, NC), and purchased from Integrated DNA Technologies (Coralville, IA). Phosphorodiamidate morpholino oligonucleotides were synthesized by Gene-Tools LLC (Philomath, OR). DNA sequencing was performed by MacrogenUSA, Inc (Rockville, MD).

Molecular biology

5′ Rapid amplification of sea urchin cDNA ends, RT-PCR of RNA from sea urchin eggs, the construction of human dysferlin-Venus and -3HA vectors, and the synthesis of mRNA from these vectors were performed using standard molecular techniques. HeLa cells were cultured using standard tissue culture techniques.

Obtaining and handling gametes

Sea urchins, *Strongylocentrotus purpuratus* or *Lytechinus variegatus* were obtained and maintained in artificial seawater (ASW) in marine aquaria as previously described (Covian-Nares et al., 2008). Eggs and sperm were obtained and fertilized as previously described (Vogel et al., 1999).

Microinjection of Calcium Green-1 dextran, morpholinos and mRNA

Sea urchin eggs were attached to 35 mm glass-bottom culture dishes that had been treated with a 1% solution of poly-D-lysine [Sigma; mol. wt. (MW) >300,000]. Attached eggs were fertilized with a 1:1000 dilution of sperm in ASW, for 1 minute and then washed with ASW. Fertilized eggs at the 1-cell stage were injected with a stock solution of either 5 mg/ml CGD (10,000 MW) in distilled water, or with a CGD stock solution supplemented with phosphorodiamidate morpholino oligonucleotides (1 mM) using an Eppendorf microinjector as previously reported (Covian-Nares et al., 2008). Injection pressure (450-550 kPa) and duration (0.6-0.9 seconds) were calibrated using Cascade blue dextran (0.1 mg/ml) to deliver approximately a 1-3% cell volume. The following three morpholinos were tested: antisense sea urchin dysferlin morpholino (5′-TCCACTGGTTTTATCGTCACT-CATC-3′), sense dysferlin morpholino (5′-GATGAGTGACGATAAAACCAG-TGGA-3′), and a random 25-base pair negative control morpholino. To rescue the inhibition of intercellular signaling caused by microinjection of antisense dysferlin morpholinos, mRNA encoding 3HA-tagged human dysferlin (0.24 μg/μl) was added to the CGD-morpholino stock solution. Following microinjection, embryos were incubated for approximately 2-3 hours at 22°C to allow them to reach at least the four-cell stage.

Multiphoton microscopy and laser wounding

Multiphoton microscopy of sea urchin embryos was performed using a Zeiss 510 META/NLO scan head attached to an upright Zeiss Axioplan 2 microscope. Ca^{2+} imaging was performed using a Zeiss Achroplan ×20, NA 0.5 water objective. CGD-injected cells were excited with 800 nm laser pulses and imaged using a 535-590 nm IR blocking band-pass emission filter, whereas scanning DIC images were acquired using a detector placed in the transmitted light path. For simultaneous imaging of embryos that were microinjected with CGD and stained with FM 4-64 (used at 4 μM) cells were excited at 800 nm and imaged using a 500-550 nm IR blocking band-pass emission filter for CGD, and a 650-710 nm IR-blocking band-pass emission filter for FM 4-64 with a 545 nm dichroic beam splitter.

Plasma-membrane laser wounding was performed using short, high intensity Ti:Sapphire laser pulses at 800 nm as previously described (Bansal et al., 2003; McNeil et al., 2003). Deleterious effects on cell function were not observed (see supplementary material Fig. S3). Images were acquired every 2 seconds before and after laser wounding. Mean intensity fluorescence timecourse plots from regions of interest were generated using Zeiss software. The change of CGD fluorescence normalized to the initial CGD fluorescence intensity ($\Delta F/F$) was calculated and plotted using Igor-Pro 6 (Wavemetrics). In some experiments inhibitors of VGCCs (cadmium, nifedipine, ω-conotoxin GVIA and ω-agatoxin IVA) or apyrase, an enzyme that catalyzes the hydrolysis of ATP and ADP to AMP, were added to the ASW.

Nucleotide perfusion experiments were performed in 35 mm glass-bottomed culture dishes. Embryos were attached to poly-D-lysine treated glass dishes. Following microinjection and incubation, the dish containing attached embryos was mounted on the microscope stage and perfused at a rate of ~1-2 ml/min with ASW or Ca^{2+}-free ASW as indicated. ASW with either 1 mM ATP, ADP or AMP was perfused over the embryos using a gravity-driven perfusion system. Lag times between switching valves and observing changes in CGD fluorescence was typically less than 1 minute. Conotoxin and agatoxin were purchased from Alamone labs. Apyrase, $CdCl_2$, ATP, ADP and AMP were purchased from Sigma.

ATP luciferase assay

Washed, packed embryos (100 µl) were added to 500 µl of ASW, ASW containing KCl (50 mM final concentration), or ASW with both KCl (50 mM) and $CdCl_2$ (500 µM final concentration) and incubated for 1 minute. Embryos were next removed and the isolated supernatants from all three samples were adjusted to a final concentration of 50 mM KCl, and 500 µM $CdCl_2$. Aliquots of these samples (50 µl) were assayed for ATP concentration using an adenosine 5′-triphosphate bioluminescent assay kit as per the manufacturer's instructions (Sigma). The integrated firefly luciferase bioluminescence signal was measured over a 3 second exposure time in 96-well plates using a Berthold Centro LB 960 luminometer. Background signal from an ASW-ATP assay mix control was subtracted from all experimental measurements.

3HA immunocytochemistry

Transfected HeLa cells were washed three times with Dulbecco's phosphate-buffered saline (DPBS; Invitrogen). The monolayer was incubated at room temperature (RT) for 20 minutes in blocking buffer (DPBS plus 10% FBS). After removal of blocking buffer the cell monolayer was incubated for 20 minutes at RT with a 1:100 dilution of anti-hemagglutinin–Alexa-Fluor-594 conjugate (HA-AF594) antibody in blocking buffer. Finally, the monolayer is washed three times with blocking buffer and placed in PBS containing Ca^{2+} and Mg^{2+} prior to imaging.

Immuno- and colocalization of dysferlin-Venus and dysferlin-3HA

Transfected cells were imaged using a Nikon ×60 (1.4 NA oil) objective mounted on a Nikon TE-2000U fluorescence microscope with a Hamamatsu ORCA-ER CCD camera driven by Velocity software (Improvision). A red filter cube (TRITC HQ exciter: 530-560 nm; dichroic: 570 nm LP; emitter: 590-650 nm) was used to image Alexa Fluor 594 fluorescence. A yellow filter cube (Yel GFP HQ exciter: 490-510 nm; dichroic: 515 nm LP; emitter: 520-550 nm) was used to image Venus fluorescence. Bright-field images were collected with a 50 msecond exposure time, and Venus and Alexa Fluor 594 fluorescence images were both collected using 5 second exposure times. Images were exported as 16-bit tiff files and processed using ImageJ.

Statistical analysis

95% confidence intervals were calculated using the modified Wald method. Analysis of 2×2 contingency tables was performed using a two-sided Fisher's exact test. All statistical calculations were performed using GraphPad Prism 5.0 software.

This work was supported by the intramural program of the National Institutes of Health, National Institute on Alcohol Abuse and Alcoholism, Bethesda, MD 20892, and by a generous gift from the Jain Foundation. Deposited in PMC for release after 12 months.

Supplementary material available online at
http://jcs.biologists.org/cgi/content/full/123/11/1884/DC1

References

Angerer, L. M. and Angerer, R. C. (2004). Disruption of gene function using antisense morpholinos. In *Development of Sea Urchins, Ascidians, and other Invertebrate Deuterosomes: Experimental Approaches*, vol. 74 (ed. C. A. Ettensohn, G. M. Wessel and G. A. Wray), p. 883. Amsterdam: Elsevier.

Anselmi, F., Hernandez, V. H., Crispino, G., Seydel, A., Ortolano, S., Roper, S. D., Kessaris, N., Richardson, W., Rickheit, G., Filippov, M. A. et al. (2008). ATP release through connexin hemichannels and gap junction transfer of second messengers propagate Ca2+ signals across the inner ear. *Proc. Natl. Acad. Sci. USA* **105**, 18770-18775.

Aoki, M., Liu, J., Richard, I., Bashir, R., Britton, S., Keers, S. M., Oeltjen, J., Brown, H. E., Marchand, S., Bourg, N. et al. (2001). Genomic organization of the dysferlin gene and novel mutations in Miyoshi myopathy. *Neurology* **57**, 271-278.

Bansal, D., Miyake, K., Vogel, S. S., Groh, S., Chen, C. C., Williamson, R., McNeil, P. L. and Campbell, K. P. (2003). Defective membrane repair in dysferlin-deficient muscular dystrophy. *Nature* **423**, 168-172.

Bashir, R., Strachan, T., Keers, S., Stephenson, A., Mahjneh, I., Marconi, G., Nashef, L. and Bushby, K. M. (1994). A gene for autosomal recessive limb-girdle muscular dystrophy maps to chromosome 2p. *Hum. Mol. Genet.* **3**, 455-457.

Bi, G. Q., Alderton, J. M. and Steinhardt, R. A. (1995). Calcium-regulated exocytosis is required for cell membrane resealing. *J. Cell Biol.* **131**, 1747-1758.

Boyd, I. A. and Forrester, T. (1968). The release of adenosine triphosphate from frog skeletal muscle in vitro. *J. Physiol.* **199**, 115-135.

Burnstock, G. (2006). Purinergic signalling. *Br. J. Pharmacol.* **147 Suppl. 1**, S172-S181.

Chiu, Y. H., Hornsey, M. A., Klinge, L., Jorgensen, L. H., Laval, S. H., Charlton, R., Barresi, R., Straub, V., Lochmuller, H. and Bushby, K. (2009). Attenuated muscle regeneration is a key factor in dysferlin deficient muscular dystrophy. *Hum. Mol. Genet.* **18**, 1976-1989.

Covian-Nares, J. F., Smith, R. M. and Vogel, S. S. (2008). Two independent forms of endocytosis maintain embryonic cell surface homeostasis during early development. *Dev. Biol.* **316**, 135-148.

Douglas, W. W. and Poisner, A. M. (1966). Evidence that the secreting adrenal chromaffin cell releases catecholamines directly from ATP-rich granules. *J. Physiol.* **183**, 236-248.

Fein, A. and Terasaki, M. (2005). Rapid increase in plasma membrane chloride permeability during wound resealing in starfish oocytes. *J. Gen. Physiol.* **126**, 151-159.

Glover, L. and Brown, R. H., Jr (2007). Dysferlin in membrane trafficking and patch repair. *Traffic* **8**, 785-794.

Jaffe, L. A. and Robinson, K. R. (1978). Membrane potential of the unfertilized sea urchin egg. *Dev. Biol.* **62**, 215-228.

Jorgensen, N. R., Henriksen, Z., Brot, C., Eriksen, E. F., Sorensen, O. H., Civitelli, R. and Steinberg, T. H. (2000). Human osteoblastic cells propagate intercellular calcium signals by two different mechanisms. *J. Bone Miner. Res.* **15**, 1024-1032.

Koopman, R. and van Loon, L. J. C. (2009). Aging, exercise, and muscle protein metabolism. *J. Appl. Physiol.* **106**, 2040-2048.

Lennon, N. J., Kho, A., Bacskai, B. J., Perlmutter, S. L., Hyman, B. T. and Brown, R. H., Jr (2003). Dysferlin interacts with annexins A1 and A2 and mediates sarcolemmal wound-healing. *J. Biol. Chem.* **278**, 50466-50473.

Liu, J., Aoki, M., Illa, I., Wu, C., Fardeau, M., Angelini, C., Serrano, C., Urtizberea, J. A., Hentati, F., Hamida, M. B. et al. (1998). Dysferlin, a novel skeletal muscle gene, is mutated in Miyoshi myopathy and limb girdle muscular dystrophy. *Nat. Genet.* **20**, 31-36.

McNeil, P. L. and Kirchhausen, T. (2005). An emergency response team for membrane repair. *Nat. Rev. Mol. Cell Biol.* **6**, 499-505.

McNeil, P. L., Miyake, K. and Vogel, S. S. (2003). The endomembrane requirement for cell surface repair. *Proc. Natl. Acad. Sci. USA* **100**, 4592-4597.

Miyake, K. and McNeil, P. L. (1995). Vesicle accumulation and exocytosis at sites of plasma membrane disruption. *J. Cell Biol.* **131**, 1737-1745.

Morel, N. and Meunier, F. M. (1981). Simultaneous release of acetylcholine and ATP from stimulated cholinergic synaptosomes. *J. Neurochem.* **36**, 1766-1773.

Nagai, T., Ibata, K., Park, E. S., Kubota, M., Mikoshiba, K. and Miyawaki, A. (2002). A variant of yellow fluorescent protein with fast and efficient maturation for cell-biological applications. *Nat. Biotechnol.* **20**, 87-90.

Neu, C. M., Rauch, F., Rittweger, J., Manz, F. and Schoenau, E. (2002). Influence of puberty on muscle development at the forearm. *Am. J. Physiol. Endocrinol. Metab.* **283**, E103-E107.

Pangrsic, T., Potokar, M., Stenovec, M., Kreft, M., Fabbretti, E., Nistri, A., Pryazhnikov, E., Khiroug, L., Giniatullin, R. and Zorec, R. (2007). Exocytotic release of ATP from cultured astrocytes. *J. Biol. Chem.* **282**, 28749-28758.

Ramakrishnan, N. A., Drescher, M. J. and Drescher, D. G. (2009). Direct interaction of otoferlin with syntaxin 1A, SNAP-25, and the L-type voltage-gated calcium channel CaV1.3. *J. Biol. Chem.* **284**, 1364-1372.

Roux, I., Safieddine, S., Nouvian, R., Grati, M., Simmler, M. C., Bahloul, A., Perfettini, I., Le Gall, M., Rostaing, P., Hamard, G. et al. (2006). Otoferlin, defective in a human deafness form, is essential for exocytosis at the auditory ribbon synapse. *Cell* **127**, 277-289.

Smith, R. M., Baibakov, B., Ikebuchi, Y., White, B. H., Lambert, N. A., Kaczmarek, L. K. and Vogel, S. S. (2000). Exocytotic insertion of calcium channels constrains compensatory endocytosis to sites of exocytosis. *J. Cell Biol.* **148**, 755-768.

Sodergren, E., Weinstock, G. M., Davidson, E. H., Cameron, R. A., Gibbs, R. A., Angerer, R. C., Angerer, L. M., Arnone, M. I., Burgess, D. R., Burke, R. D. et al. (2006). The genome of the sea urchin Strongylocentrotus purpuratus. *Science* **314**, 941-952.

Terasaki, M., Miyake, K. and McNeil, P. L. (1997). Large plasma membrane disruptions are rapidly resealed by Ca^{2+}-dependent vesicle-vesicle fusion events. *J. Cell Biol.* **139**, 63-74.

Vogel, S. S., Smith, R. M., Baibakov, B., Ikebuchi, Y. and Lambert, N. A. (1999). Calcium influx is required for endocytotic membrane retrieval. *Proc. Natl. Acad. Sci. USA* **96**, 5019-5024.

Washington, N. L. and Ward, S. (2006). FER-1 regulates Ca^{2+}-mediated membrane fusion during C. elegans spermatogenesis. *J. Cell Sci.* **119**, 2552-2562.

Whitaker, M. (2006). Calcium at fertilization and in early development. *Physiol. Rev.* **86**, 25-88.